A WPT-Enabled UAV-Assisted Condition Monitoring Scheme for Wireless Sensor Networks

Tharindu Dilshan Ponnimbaduge Perera, *Graduate Student Member, IEEE*, Stefan Panic, *Member, IEEE*, Dushantha Nalin K. Jayakody, *Senior Member, IEEE*, P. Muthuchidambaranathan, *Member, IEEE*, and Jun Li, *Senior Member, IEEE*

***Abstract*— In this paper, a resource allocation and data gathering scenario of an unmanned aerial vehicle (UAV) assisted wireless powered sensor network is investigated, in which the sensor nodes (SNs) are remotely powered by power beacons (PBs) via radio-frequency wireless power transmission (RF-WPT). A time-block structure with two phases is proposed to accommodate operations in the proposed system. During Phase-I, SNs harvest energy from PBs and periodically send its sensed data to the selected cluster heads (CHs). In Phase-II, an UAV collects the data from CHs to be delivered to the data sink for further processing avoiding the need for long range transmission and multi hop communication to the data sink. Then, a closed-form expression for outage probability of the proposed system over Rayleigh and Rician fading channels is derived. Next, outage probability minimization problem is formulated to obtain optimal time allocation for RF-WPT energy harvesting to improve the system performance. Due to the complexity of the problem, Lagrangian duality method is used to develop an asymptotic optimal solution with less execution complexity avoiding complex brute force/ exhaustive search approach. Furthermore, a heuristic method is presented to further lower the computation complexity. Simulation results reveal the superiority of the proposed methods compare to brute force/ exhaustive search approach via analysis, comparison and insights of the system performance results. Finally, the performance superiority of the proposed system is demonstrated with compare to identified baseline WSNs.**

***Index Terms*— RF energy harvesting, RF wireless power transfer, UAV communication, wireless sensor networks and 5G communication.**

Manuscript received March 31, 2020; revised June 23, 2020; accepted July 30, 2020. This work was supported in part by the Russian Foundation for Basic Research (RFBR) under Grant 19-37-90037, in part by the framework of the Competitiveness Enhancement Program of the National Research Tomsk Polytechnic University, Russia, under Grant VIU-ISHITR-180/2020, and in part by the Scheme for Promotion of Academic and Research Collaboration (SPARC), Ministry of Human Resource Development, India, under Grant SPARC/2018 – 2019/$P145/SL$. The work of Jun Li was supported in part by the National Key Research and Development Program under Grant 2018YFB1004800 and in part by the National Natural Science Foundation of China under Grant 61727802 and Grant 61872184. The Associate Editor for this article was M. Guizani. *(Corresponding authors: Dushantha Nalin K. Jayakody; Jun Li.)*

Tharindu Dilshan Ponnimbaduge Perera and Stefan Panic are with the School of Computer Science and Robotics, National Research Tomsk Polytechnic University, 634050 Tomsk, Russia (e-mail: ponnimbaduge@tpu.ru; stefanpnc@tpu.ru).

Dushantha Nalin K. Jayakody is with the School of Computer Science and Robotics, National Research Tomsk Polytechnic University, 634050 Tomsk, Russia, and also with the Centre for Telecommunication Research, School of Engineering, Sri Lanka Technological Campus, Padukka 10500, Sri Lanka (e-mail: nalin@tpu.ru).

P. Muthuchidambaranathan is with the Department of Electronics and Communication Engineering, National Institute of Technology Tiruchirappalli, Tiruchirappalli 620015, India (e-mail: muthuc@nitt.edu).

Jun Li is with the School of Electronic and Optical Engineering, Nanjing University of Science and Technology, Nanjing 210094, China (e-mail: jun.li@njust.edu.cn).

Digital Object Identifier 10.1109/TITS.2020.3018493

I. Introduction

ADVANCES in fifth generation and beyond (5GB) communication networks are designed to accommodate emerging technologies such as Internet-of-Things (IoT), to increase new innovations across various industries. Operationally advanced IoT services are empowered by using massive number of sensor nodes (SNs) in wireless sensor networks (WSNs). Multiple groups of SNs, which are positioned in the field-of-interest are used to sense the environmental conditions of special events and hard-to-reach locations such as natural disasters, agricultural fields, smart cities, volcanic environments, natural gas reservoirs etc. A sensor node (SN) is composed of multiple sensors to detect specific changes in the surrounding environment, which are later to be delivered to data sinks for further processing. However, these SNs are significantly constrained in terms of its battery life, limiting the operational capabilities of the WSN and achievable quality of service (QoS). Hence, a significant number of different energy-aware protocols have been proposed to minimize energy consumption in order to improve the lifetime of WSNs. Nevertheless, current energy-aware protocols unable to achieve uninterrupted long-term operations for the WSNs [1]. Thus, energy harvesting (EH) techniques have been applied to WSNs enabling SNs to powered-up or replenish its inbuilt batteries from ambient sources [2]. However, in general, ambient energy sources i.e., solar, wind, are unable to power-up WSNs continuously, even after adopting effective energy allocation and management schemes [3]. To overcome the aforementioned drawbacks, a new EH technique named radio frequency wireless power transfer (RF-WPT) has emerged to power-up WSNs. RF-WPT is reliable and stable compare to ambient energy sources. Thus, EH from RF-WPT is suitable for low power energy constrained communication networks such as WSNs, to increase the overall operational time uninterruptedly [1], [2]. RF-WPT is investigated in open literature

along with recent advances in wireless communication systems, cf. [2].

In recent decade, RF-WPT applied WSNs have been investigated extensively to improve operational time of the communication systems [4]–[9]. The simulation for a complete system of RF-WPT is used to energized SNs of WSN in [4]. In addition, the authors of [4] were implemented a prototype to identify the difference between simulation and the real world applications. The authors of [5] implemented a RF energy harvester made of compact ferrite rod antenna together with rectenna, in principle, to power-up SNs within 120 km of 150 kW transmitter. In [6], the authors aimed to optimize the power allocation strategy in priority constraint RF-WPT system with a large number of SNs in cognitive IoT. The authors proposed a critical path based decomposition strategy with low computational complexity. A selective, tracking and power adaptive far-field RF-WPT system, which can integrate into passive WSNs proposed in [7]. Furthermore, the authors have shown that effective far-field RF-WPT links can be created with reasonable simplicity making RF-WPT a competitive candidate for energy constrained problem in WSNs. The authors of [8] presented RF-WPT and intelligent routing modules to preserve energy consumption and lifetime of SNs. The authors exploited wireless power charging device to solve the multi-objective function for charging trails. By considering downlink RF-WPT and uplink information transmission, the authors of [9] established a task processing strategy including uplink and downlink power information dynamic time division. Furthermore, it is shown that the down going energy transmission can effectively improve the average received power maximizing the throughput.

In most of the WSN applications, SNs are required to send collected sensor observations directly or through multiple hops to data sinks for further processing. Thus, there is a requirement for an innovative new design of data collection strategy to enhance the scalability and the performance of the WSN. Recently, unmanned aerial vehicle (UAV) is identified as an effective application to collect data from SNs located in hard-to-reach environments, when there are no feasible connections towards data sinks [10]. As Compared to conventional WSNs that depend on static data collecting nodes or multi-hop data relaying, the UAV can directly communicate with the SN exploiting favourable LoS dominant air-to-ground channels. Furthermore, UAVs are help to increase coverage area and sum-throughput of the WSNs while reducing the overall energy consumption of the WSNs [11], [12].

Various applications of UAV-aided WSNs have been investigated in the literature [13]–[18]. A UAV-aided data collection scheme for wireless powered WSN over Rician fading channels is developed in [13]. The authors analyzed the outage probability of the proposed system under the assumption of Rician fading channels and demonstrated that for the given information rate, outage probability threshold and UAV location, the achievable service range can be uniquely determined. In [14], the authors have jointly optimized the SNs' wake up schedule and UAV's trajectory to minimize the energy consumption of each SN. This proposed scheme achieved significant energy savings compared to its benchmark schemes i.e., static collection and direct trajectory. A novel data acquisition framework in WSN using UAV is proposed in [15] to increase the efficiency of data gathering process. The authors have introduced a priority based frame selection scheme to reduce the number of redundant data transmission between SNs and the UAV. The UAV aided data collection strategy for a SNs located in a straight line has been studied in [16]. Here the aviation time of the UAV can be minimized by following classical water filling policy for optimal power allocation.

If all SNs transmit the sensed data to the data sink with the aid of an UAV, energy efficiency of the entire system can be decreased in a considerable amount causing decrease in QoS. Generally, neighbouring SNs have the similar data since each group of SNs collect information within a specific area [16]. In addition, collecting data from each SN in a large scale WSN using UAV can be practically infeasible due to UAV's limited inbuilt battery capacity. Thus, as a solution for the aforementioned problems, a cluster head (CH) is selected from each cluster of SNs in the WSN. CHs received the data from SNs in the matching cluster and then UAV collects the data from the CHs in order to be conveyed to the data sink. Thus, the selection of CH for a given cluster is one of the vital problem in WSNs, which affects the overall system performance. In order to overcome unreasonable CH selections and excessive energy consumption, a modified CH selection algorithm based on LEACH was proposed in [17]. Furthermore, the authors managed to balance the network energy burden and improved energy efficiency by leveraging CH competitive mechanism in the proposed algorithm. In [18], firefly with cyclic randomization is proposed for CH selection to improve communication network performance. In [19], the authors have proposed CH selection scheme that rotates the CH position among the SNs with higher energy levels as compared to other.

However, [4-16] have not focused on the combination of RF-WPT, UAV aided data collection strategy and the performance metrics at the data sinks in a WSN while considering possibility of occupying different types of fading channels within the communication network, which can resemble a real world practical scenario in IoT applications. RF-WPT is a potential and effective candidate to reduce carbon footprint in IoT applications [20]. Following are the identified advantages of RF-WPT for future IoT applications, i.e. 1). RF-WPT acts as a bridge between green energy sources and communication devices, 2). The energy harvested via RF-WPT at a receiver is foreseeable, 3). The amount of harvested energy depends upon to transmit power, propagation loss, and wavelength. In addition, the rapid advances in intelligent transportation systems (ITS) have led to a rapid expansion in condition monitoring of communication systems, infrastructures, vehicles, and machinery using SNs [21]. Thus, in this work, an energy efficient UAV-aided data collection strategy for wireless powered WSN is proposed and the system performance is investigated in terms of outage probability and achievable throughput at the data sink. In particular, this work aims at introducing a framework to realize the integration of WPT, UAV into WSNs to improve overall energy efficiency of

IoT applications such as ITS, smart cities, etc. while maintaining the expected QoS. The main contributions of the paper are fourfold, which are summarized as follows.

- First, a wireless powered WSN is designed, in which SNs are remotely powered by the PBs using RF-WPT. A new time-block structure is presented by dividing entire operational time into two phases. In the first phase, WSN is clustered, an optimal CHs are selected within the powered-up SNs and each SNs periodically sends its sensed data to CHs. In the second phase, an UAV used to increase energy level of CH via RF-WPT and collects the aggregated data from the CHs.
- Secondly, under the assumption of Rayleigh and Rician fading channels, the outage probability at the data sink is derived. Then an optimization problem is formulated to quantify the time allocation for EH that minimizes the outage probability subject to SNs transmit power, harvested energy and UAV's trajectory constraints.
- Thirdly, an asymptotic optimal solution is proposed by considering the duality of the formulated optimization problem to reduce the complexity as compare to brute-force or exhaustive search mechanism. Then, a heuristic solutions for clustering, CH selection and UAV's trajectory is presented to further reduce the complexity.
- Finally, the effectiveness of proposed asymptotic and heuristic solutions for the formulated problem, in comparison to the existing traditional brute-force is demonstrated by the aid of simulation results. Furthermore, the impacts of different system parameters to the overall system performance are investigated. Finally, the performance superiority of the proposed WSN is demonstrated compare to the benchmark WSNs.

The remainder of this paper is organized as follows. The Section II depicts the system model and the time block structure. Section III offers detail derivation of the outage probability of the system. The problem formulation for outage minimization is provided in Section IV. The proposed asymptotic and heuristic solutions are given in Section V and VI, respectively. Simulation results are provided in Section VII, followed the conclusion.

II. System Model

A UAV-aided WSN is considered in this paper as illustrated in Fig. 1 with a UAV flying over N number of SNs and collecting data from the selected CHs within a given time period of T. M PBs are randomly deployed within the WSN to power-up the SNs. Initially, all SNs do not have energy in their rechargeable batteries to transmit sensed data. A reference WSN is illustrated in Fig. 1(a), where the UAV's starting and ending points are represented by S and D and SNs are denoted by circles, respectively. It is assumed that the location D represents the desired data sink where sensor observations are intended to be delivered for further processing. It is also noteworthy that the S and D are not fixed and can position in different locations depending on the structure of the WSN. It is also noteworthy that in practice, the start and final locations of the UAV depend on multiple factors such as UAV take-off and landing locations, post-mission flying paths, the capacity of the UAV's battery, etc.

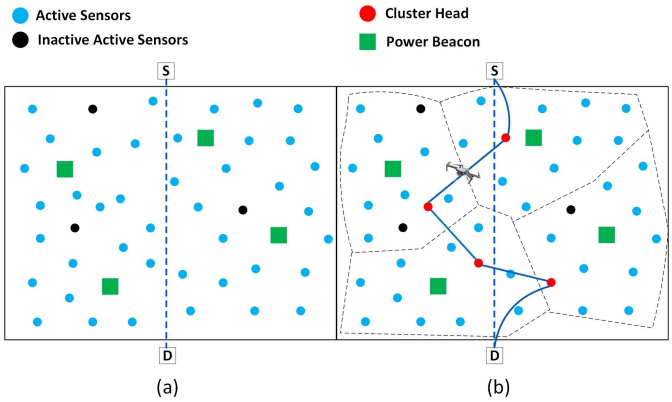

Fig. 1. Illustration of reference UAV aided data collection in WSN. (a) Sample WSN with randomly distributed SNs and PBs. (b) Sample output of the proposed data gathering scheme in Phase II with four clusters (separated with dotted lines), selected CHs and projected UAV trajectory.

A time-block structure for the data collection process of the proposed WSN is illustrated in Fig. 2. Entire operational time T is partitioned into two phases $T\alpha$ and $T(1-\alpha)$, where $0 < \alpha < 1$. Phase-I is further divided into another two fractions $T\alpha\tau$ and $T\alpha(1-\tau)$. During the time $T\alpha\tau$, all SNs harvest energy from the RF-WPT signals received from PBs to recharge their batteries. Then, in the next time fraction $T\alpha(1-\tau)$, SNs are grouped into clusters, an optimal CH is selected for each clusters and then, SNs transmit the sensed data to the respective CH. Time allocated for Phase-II is equally divided into M number of clusters which can be represented as $T(1-\alpha)/M$. Then the time fraction $T(1-\alpha)/M$ is further divided into two time slots $F\beta$ and $F(1-\beta)$, where $F = T(1-\alpha)/M$ and $0 \leq \beta < 1$. During the time slot $F(1-\beta)$, CH harvests energy from RF-WPT signal of the UAV. Then, CH transmits the aggregated data to the UAV in order to be sent to the data sink for further processing. The channel coefficients between SNs-PBs and SNs-CHs are modeled as Rayleigh fading random variable h_{xy} from node x to y, where $x, y \in \{n, j\}$. The LoS channel between the UAV and the CHs are modeled using Rician fading random variable g_{xy}, where $x, y \in \{m, u\}$.

It is assumed that the data transmission from each SN to CH is orthogonal[1] as in [22] to avoid interference with each other's transmission. Thus, it is possible to have multiple SNs to transmit data in same time slot to the CHs as long as they do not conflict with each other. Similarly, it is assumed that the CHs are not transmitting simultaneously to the UAV avoiding interference with each other. We have consider two minimum SNR threshold values γ_1 and γ_2 for the received signals at the CHs and the UAV to maintain the expected QoS, respectively. This is mainly due to the difference within the weight of received information at the CHs and the UAV. At the beginning, the UAV works out its trajectory and communication schedule for CHs using the knowledge of its

[1]Orthogonality can be achieved in various ways, i.e. by performing Orthogonal frequency-division multiple access (OFDMA) or Time-division multiple access (TDMA) approach.

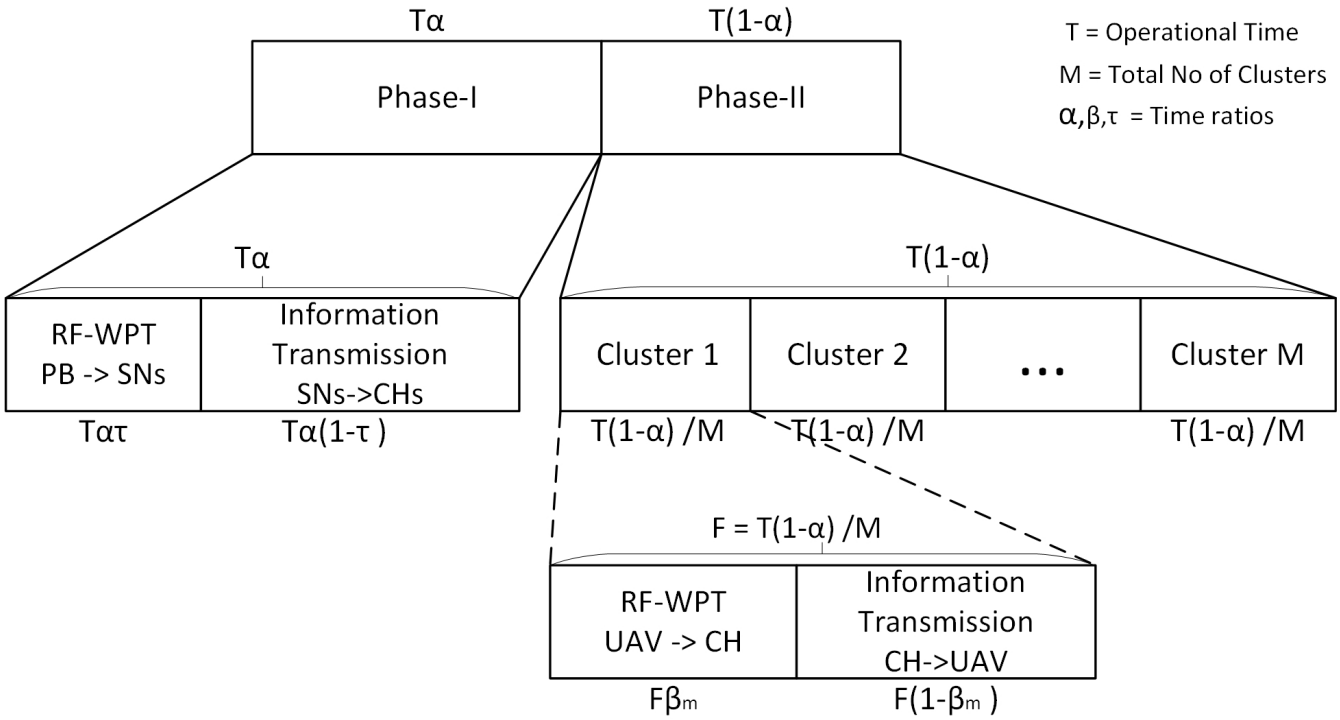

Fig. 2. Time allocation diagram of the proposed WSN, where total operational time is divide into two phases. Time allocation for energy harvesting process for SNs and CHs denote by τ and β.

locality with the CHs along with the trajectory. Furthermore, CHs' locations and energy level are assumed to be known at the UAV. The details of such approach can be found in [23].

A. Phase-I

Let P_j denotes the transmission power of the j^{th} PB during the time $T\alpha\tau$, where $j \in \{1, .., M\}$. Assuming that the transmitted RF-WPT signals by PBs are mutually independent as in [22], the total harvested energy at the n^{th} SN can be expressed as

$$E_n = \sum_{j=1}^{M} E_{nj} = \sum_{j=1}^{M} P_j d_{nj}^{\omega} \eta_n |h_{nj}|^2 T\alpha\tau, \tag{1}$$

where d_{nj} denotes the distance between n^{th} SN and j^{th} PB, ω represents the path-loss exponent and $0 < \eta_n < 1$ is the energy conversion efficiency at the n^{th} SN. After SNs energized its rechargeable batteries, SNs sense data from the surrounding environment. The transmit power of the each SN during the Phase-I can be given by

$$P_n = \frac{E_n}{T\alpha(1-\tau)} = \sum_{j=1}^{M} \frac{P_j d_{nj}^{\omega} \eta_n |h_{nj}|^2 \tau}{(1-\tau)}. \tag{2}$$

Therefore, the received signals by the CH at the end of Phase-I can be expressed as

$$y_m = \sum_{n=1}^{J-1} \sqrt{P_n} |h_{mn}| s_n + n_{mn}, \tag{3}$$

where $m \in \{1, \ldots, M\}$ is the index of the clusters in the WSN, $J = N/M$ denotes the number of SNs per each cluster, h_{mn} denotes the channel coefficient between SN n and the CH of cluster m, s_n denotes the normalized modulated signal transmitted from SN n with the value $\mathbb{E}[|s_n|^2] = 1$ and n_{mn} represents the AWGN noise between the SN n and the respective CH. Thus, by considering (1) and (2), the effective signal-to-noise ratio (SNR) at the CH in cluster m can be given as

$$\gamma_m = \sum_{n=1}^{J-1} \frac{P_j d_{nj}^{\omega} |h_{nj}|^2 |h_{mn}|^2 \tau}{(1-\tau)\sigma_{mn}^2}. \tag{4}$$

B. Phase-II

At the beginning of the Phase-II, CHs possess the aggregated data received from the SNs during the Phase-I. During the time slot $F\beta$, CH in m^{th} cluster harvests energy from the UAV's RF-WPT signal. Thus, the amount of energy harvested by the CH can be expressed as

$$E_{mu} = \left\{ \begin{array}{ll} P_u \eta_n |g_{mu}|^2 \rho_u F\beta, & \text{if } E_{mu} < E_{max} \\ 0, & \text{otherwise} \end{array} \right\} \tag{5}$$

where P_u denotes the RF-WPT transmission power of the UAV, $F = T(1-\alpha)/M$, g_{mu} represents the complex fading coefficient between the UAV and CH, $\rho_u = \kappa d_{mu}^{\omega}$ denotes the pathloss between UAV and CH, where κ is the constant coefficient of the pathloss and d_{mu} is the LoS distance between UAV and the CH. It is also noteworthy that the $d_{mu} = H_{min}$ during the time when UAV is hovering on top of the CH. Also it is assumed that the H_{min} is the minimum altitude required for maneuvering without any terrain blockage and it complies with the municipal rules and regulations of the area. Thus,

the total energy available in CH to use for data transmission can be calculated by adding (3) and (4).[2] The received signal at the UAV from the CH of cluster m can be written as

$$y_u^m = \sqrt{P_n^m}|g_{um}|\rho_u(y_m) + n_{um}, \tag{6}$$

where P_n^m denotes the transmission power of the CH in cluster m, g_{um} represents the complex fading coefficient between CH in m and the UAV and n_{um} denotes the AWGN noise between CH and the UAV. Then, the end-to-end SNR can be written as

$$\gamma_u^m = \frac{P_m|g_{um}|^2\rho_u^2\sum_{m=1}^{J-1}P_n|h_{mn}|^2}{P_m|g_{um}|^2\rho_u^2\sigma_{mn}^2+\sigma_{um}^2}. \tag{7}$$

By substituting (2), (4) and (5) into (7) SNR at the UAV at the end of data collecting from CH in cluster m can be arrange as in (8) given in bottom of the page, where $a_1 = \frac{P_j d_{nj}^{\omega}\alpha\tau M\eta_n^2+\rho_u^2}{(1-\alpha)(1-\tau)(1-\beta)}\frac{P_u\rho_u(1-\alpha)\beta}{}$, $a_2 = a1\kappa^2$, $a_3 = \frac{\eta_n P_j d_{nj}^{\omega}\alpha\tau\rho_u}{(1-\alpha)(1-\beta)}$.

III. Outage Probability Analysis

In this paper, a delay-limited transmission mode is considered.[3] Thus, in this section, detailed derivation of outage probability of the proposed system is provided. Let us observe the random variables X_1, X_2 and X_3 denoting squares of channel gain amplitudes represent in (8), where $X_1 = |g_{u,m}|^4$, $X_2 = |h_{m,n}|^2$ and $X_3 = |h_{n,j}|^2$. In this work, the outage probability within a single cluster is defined as the probability that the end-to-end SNR at the UAV falls under a desired threshold SNR value γ_2, which can be expressed as

$$P_r\left(\frac{a_1X_1X_2X_3}{a_2X_1X_2X_3+a_3\sqrt{X_1}X_3+\sqrt{X_1}\rho_u\sigma_u^2+\sigma_u^2} \le \gamma_2\right), \tag{9}$$

or equivalently

$$P_r\left(X_2 \le \frac{\gamma_2a_3\sqrt{X_1}+\gamma_2\sqrt{X_1}\rho_u\sigma_u^2+\gamma_2\sigma_u^2}{X_1X_3(a_1-a_2\gamma_2)}\right), \tag{10}$$

with the assumption of $(a_1 - a_2\gamma_2 > 0)$, which is feasible in practical scenario [26]. Therefore, Outage probability of the cluster m, where $m = \{1, \ldots, M\}$ can be calculated as

$$P_{out}^m = \int_0^\infty\int_0^\infty F_{X_2} \times\left(\frac{\gamma_2a_3\sqrt{X_1}+\gamma_2\sqrt{X_1}\rho_u\sigma_u^2+\gamma_2\sigma_u^2}{X_1X_3(a_1-a_2\gamma_2)}\right) \times f_{X_1}(X_1)f_{X_3}(X_3)dX_1dX_3, \tag{11}$$

where cumulative distribution function (CDF) $F_{X_2}(X_2)$ is follows Rayleigh distribution. Thus, probability density function (PDF) of Rayleigh distributed SNR at the CH can be expressed as

$$F_{X_2}(X_2) = 1 - \exp\left(-\frac{X_2}{\Omega_{mn}}\right), \tag{12}$$

where $\Omega_{mn} = \mathbb{E}(X_2)$ denotes the average channel SNR between SNs and the CH. Similarly, PDF function $f_{X_3}(X_3)$ is Nakagami-m distributed SNR at the SN and can be expressed as

$$f_{X_3}(X_3) = \frac{X_3^{M-1}M^M\exp(-MX_3)}{\Gamma(M)\Omega_{nj}^M}, \tag{13}$$

where $\Omega_{nj}^M = \mathbb{E}(X_3)$ average channel SNR between PBs and SNs. Since each CHs receive multiple signals from SNs during the second part of the Phase I, random variable X_2 can be also written as $X_2 = \sum_{n=1}^{J-1}|h_{m,n}|^2$. Thus, sum of M number of distributed Rayleigh random variables can be expressed as Nakagami-m random process with parameter $m = M$ [26]. The PDF of X_1 is considered as double distributed Rician random variable, thus, SNR at the UAV can be expressed as

$$f_{X_1}(X_1) = 2\sum_{p=0}^{\infty}\sum_{q=0}^{\infty}\frac{(1+K_m)^{(p+q+2)}K_m^{(p+q)}\exp(-2K_m)}{\Omega_{um}^{p+q+2}\Gamma(p+1)\Gamma(q+1)p!q!} \times X_1^{\frac{p+q}{2}}K_{(p-q)}\left(2\frac{(1+K_1)}{\Omega_{um}}\sqrt{X_1}\right), \tag{14}$$

where K_m denotes the Rician K-factor, which is defined as the ratio of the power of LoS component to the scatter component, Ω_{um} denotes the average channel SNR between CH and the UAV, $K_v()$ represents the v^{th} order modified Bessel function of the second kind and $\Gamma(x)$ denotes the complete Gamma function. The double integral form in (11) could be further simplified into single integral form by integrating over X_3 variable as given in (15), shown at the bottom of the page.

[2]Note that SNs can choose to perform power control without exhausting the harvested energy as in [1], [24], which is considered as out of the scope of this paper

[3]Achievable sum-throughput can be calculated by evaluating the outage probability of the system with fixed transmission rate [25].

$$\gamma_u^m = \frac{\sum_{n=1}^{J-1}\sum_{j=1}^{M}a_1|g_{u,m}|^4|h_{n,j}|^2|h_{m,n}|^2}{\sum_{n=1}^{J-1}\sum_{j=1}^{M}|g_{u,m}|^4|h_{n,j}|^2|h_{m,n}|^2a_2+\sum_{j=1}^{M}|g_{u,m}|^2|h_{m,n}|^2a_3+|g_{u,m}|^2|\rho_u\sigma_u^2+\sigma_u^2} \tag{8}$$

$$P_{out}^m = 1 - 4\sum_{p=0}^{\infty}\sum_{q=0}^{\infty}\frac{(1+K_i)^{(p+q+2)}K_i^{(p+q)}\exp(-2K_i)M^{\frac{M}{2}}}{\Omega_{um}^{p+q+2}\Omega_{n,j}^M\Omega_{hi}^{\frac{M}{2}}\Gamma(p+1)\Gamma(q+1)p!q!}\int_0^\infty\left(\frac{\gamma_2a_3\sqrt{X_1}+\gamma_2\sqrt{X_1}\rho_u\sigma_u^2+\gamma_2\sigma_u^2}{X_1(a_1-a_2\gamma_2)}\right)^{\frac{M}{2}} \times X_1^{\frac{p+q}{2}}K_M\left(2\sqrt{\left(\frac{\gamma_2a_3\sqrt{X_1}+\gamma_2\sqrt{X_1}\rho_u\sigma_u^2+\gamma_2\sigma_u^2}{X_1(a_1-a_2\gamma_2)\Omega_{um}}M\right)}\right)K_{(p-q)}\left(2\frac{(1+K_1)}{\Omega_{um}}\sqrt{X_1}\right)dX_1 \tag{15}$$

However, to the best of the authors' knowledge, this integral cannot be further simplified into a closed-form expression. Thus, we apply Laplace approximation over the double integral form in (11) as

$$\int_0^\infty \int_0^\infty f_1(X_1, X_3) \exp\left(-\lambda f_2(X_1, X_3)\right) dX_1 dX_3 = \frac{2\pi}{\lambda} \frac{f_1(X_1(0), X_3(0))}{\sqrt{|det(H)|}} \exp\left(-\lambda f_2(X_1(0), X_3(0))\right). \quad (16)$$

where $X_1(0)$ and $X_3(0)$ are considered as positive real values obtained from the system:

$$\frac{d(f_1(X_1, X_3))}{dX_1} = 0, \quad \frac{d(f_1(X_1, X_3))}{dX_3} = 0, \quad (17)$$

while H denotes Hessian matrix of function $f_1(X_1, X_3)$ over X_1 and X_3 at points $X_1(0)$ and $X_3(0)$. Then, substituting Hessian matrix of function $f_1(X_1, X_3)$ into (16) and considering (17), the final closed-form expression of the outage probability at the UAV after receiving data from CH in cluster m can be expressed as in (18), shown at the bottom of the page.

Thus, the outage probability at the data sink can be written as

$$P_{out} = \sum_{i=1}^{M} P_{out}^m. \quad (19)$$

Based on the outage probability closed-form expression in (18), the achievable sum-throughput at the UAV for cluster m can be written as

$$R_m = (1 - P_{out}^m) RT \left(\frac{(1-\alpha)(1-\beta)}{M}\right), \quad (20)$$

where R denotes the fixed transmission rate of the CHs. Considering (19), the sum throughput at the data sink can be expressed as

$$R_t = (1 - P_{out}) RMT(1-\alpha)(1-\beta). \quad (21)$$

IV. Outage Minimization Problem Formulation

In this section, the problem of clustering, CH selection, UAV's optimal trajectory and optimal power allocation that minimizes the outage probability are considered to obtain optimal values for time ratio α, τ, β. For the proposed system, four constraints are required for the clustering process of the WSN to maintain the expected QoS. The acronyms used in this section are provided in Table I.

TABLE I
Acronyms Used in Section IV

Symbol	Definition
S	set of SNs in the WSN
A	set of active SNs in the WSN
B	set of clusters in the WSN
D	set of distance between nodes (N×N matrix)
L	set of SNs in UAV trajectory connecting starting and destination points
E_{min}	minimum amount of energy required to be an active SN
E_{max}	maximum battery capacity of the SNs
$C_{mn} \in \{0,1\}$	indicating whether SN n is a member of cluster m
$C_n^m \in \{0,1\}$	indicating whether SN n selected as CH for cluster m
$Y_{zq} \in \{0,1\}$	indicating whether UAV is traversing from SN z to q

$$E_n \geq E_{min}, \quad \begin{cases} n \in A, \\ n \notin A, \quad \text{otherwise}, \end{cases} \quad (22)$$

$$\sum_{n \in A} C_{mn}, \leq \frac{N}{M} \quad \forall m \in B, \quad (23)$$

$$\sum_{m \in B} C_{mn} = 1, \quad \forall n \in A, \quad (24)$$

$$P_j \geq \frac{\gamma_1}{\max[D]^{-\omega}} \quad j = 1, \ldots, M. \quad (25)$$

The constraint (22) asserts that after performing energy harvesting from PBs, each SN should have at least E_{min} amount of energy in the SN's battery/energy storage in order to be considered for clustering process. Otherwise, SN will be considered as an inactive SN and will not consider for clustering process. The constraint (23) enforces that no SN is belongs to more than one cluster. The symbol $C_{m,n} \in \{0, 1\}$ indicates whether the SN n is a member of cluster m and also asserts that each SN only belongs to one cluster. The constraint (25) enforces that the transmission power of the PB j is sufficient enough to harvest energy to maintain expected QoS during the information transmission to CH. Following constraints are used in the CH selection process and make sure that the optimal CH is selected in terms of system performance and UAV's trajectory.

$$C_n^m \leq C_{mn}, \quad \forall m \in B, \ \forall h \in A, \quad (26)$$

$$\sum_{h \in A} C_n^m = 1, \quad \forall m \in B, \quad (27)$$

$$E_{min}^{CH} < E_n^m, \quad \forall m \in B, \quad (28)$$

$$T_n^m = 1, \quad \forall m \in B. \quad (29)$$

$$P_{out}^m = 1 - 2 \sum_{p=0}^{\infty} \frac{(1+K_m)^{\frac{p+1}{2}} K_m^p \exp(-K_m)}{\Omega_{um} \Gamma(p+1) p!} \times \left(\frac{a_3^m \gamma_2}{(a_1^m - a_2^m \gamma_2)\Omega_{n,m}}\right)^{\frac{p-1}{2}} K_{(p-1)} \left(2\sqrt{\frac{(1+K_m))a_3^m}{(a_1^m - a_2^m \gamma_2)\Omega_{u,m}\Omega_{mn}}}\right) \quad (18)$$

The constraint (26) enforces that a SN cannot be selected as a CH if it is not in cluster m. The constraints (27) and (28) assure that there is only one CH per each cluster and a SN cannot be selected as CH if the harvested energy is less than the provided threshold value, respectively. The symbol T_n^m indicates the UAV's trajectory and constraint (29) enforces that the CH n is selected for UAVs trajectory. Following trajectory constraints ensure that the UAV starts from the selected starting point, fly over all CHs to collect data and finally arrive at the destination location as in [24], [25].

$$\sum_{z\in B_m}\sum_{(zq)\in V} Y_{z,q} = 1, \tag{30}$$

$$\sum_{z\in V} Y_{Sz} = 1, \tag{31}$$

$$\sum_{q\in V} Y_{qD} = 1, \tag{32}$$

$$\sum_{(z,q)\in V} Y_{zq} - \sum_{(q,z)\in V} Y_{qz} = \begin{Bmatrix} 1, z = S \\ -1, z = D \\ 0 \end{Bmatrix}, \tag{33}$$

$$R_z - R_q + Y_{zq}M <= M - 1. \tag{34}$$

The constraints (30), (31), (32) and (33) enforce UAV to fly from selected starting point to selected destination flying over only one CH of each cluster. Finally, constraint (34) asserts that the UAV will not get into a flying loop during the data collection. Then, the corresponding optimization problem can be mathematically expressed as

$$\begin{aligned}
(P1): \quad & \min_{\{m\in M, E_m, P_u\alpha,\tau,\beta\}} \sum_{m=1}^{M} P_{out}^m \\
& \text{subject to: } (C1): \quad E_n^m \geq \frac{\gamma_2 T(1-\alpha)(1-\beta)}{MH_{min}}, \\
& (C2): \quad E_u \geq \sum_{m=1}^{M} E_m, \\
& (C3): \quad E_n \geq \frac{\gamma_1 T\alpha\tau}{max[D]^{-\omega}}, \\
& (C4): \quad 0 < \alpha < 1, \\
& (C5): \quad 0 < \tau < 1, \\
& (C6): \quad 0 \leq \beta_m < 1, \quad \forall m \in B, \\
& (C7): \quad (22) - (29), \\
& (C8): \quad (30) - (34),
\end{aligned} \tag{35}$$

where $m = \{1, \ldots, M\}$, E_n^m denotes the amount of energy harvested by the CH, E_u represents the energy allocated for UAV's RF-WPT link to power-up CHs and E_n denotes the amount of energy harvested by SNs from RF-WPT signal received from PBs. The objective of (35) is to minimize the outage probability at the UAV by identifying optimal time ratios. Constraint (C1) make sure that each CH has harvested sufficient energy to maintain the expected QoS between CH and the UAV. Constraint (C2) represents the required amount of energy by the UAV for RF-WPT. The constraint (C3) ensures that the PBs' RF-WPT transmission power is adequate enough for SNs to harvest energy to maintain expected QoS during information transmission between SNs and CHs. This optimization problem is a non linear mixed integer programming problem involving finding optimal clustering, CH selections with joint computation of time ratios α, τ, β_m and optimal energy allocations. Due to the complexity of the formulated problem, an asymptotic solution with less complexity as compared to highly complex Brute-force/exhaustive search method is presented in the following section.

V. Asymptotic Optimal Solution

The discrete nature of the binary variables involved in clustering, CH selection and trajectory of the UAV, causes difficulties in solving the formulated problem in (35), especially when the amount of harvested energy and transmission power of the SNs and the UAV are considered. Therefore, a method that offers asymptotically optimal values for variables with minimum time complexity is required for the proposed system. By using the Lagrangian duality method adhering to the requirements of the proposed system, the formulated (P1) in (35) can be solved as follows. First, a set $\mathcal{D}$ is defined with all possible clustering $c_1 = C_{m,n}$, selected CHs $c_2 = C_n^m$, UAV's trajectory information $y = Y_{z,q}$ and time ratio $\beta = \beta_m$. The set $\mathcal{D}$ satisfies the all constraints (C6), (C7) and (C8). Thus, the corresponding Lagrangian dual function of the problem (P1) is given by

$$g(\Lambda) \triangleq \min_{\substack{\mathbf{p}\in\mathcal{P}(c_1,c_2,y,\beta) \\ (c_1,c_2,y,\beta)\in\mathcal{D}}} \mathcal{L}(p, c_1, c_2, y, \beta, \alpha, \tau; \Lambda), \tag{36}$$

where $\mathbf{p}$ denotes the set of power allocation for given set $\mathcal{P}$ of clusters, CHs, UAV trajectory and time ratio β_m. The corresponding Lagrangian expression of (36) can be expressed as

$$\begin{aligned}
\mathcal{L}(p, c_1, c_2, y, \beta, \alpha, \tau; \Lambda) = & \sum_{m=1}^{M} P_{out}^m + \lambda_u(E_u - \sum_{m=1}^{M} E_m) \\
& + \sum_{n=1}^{J} \lambda_{mn}(E_n^m - \sum_{j=1}^{M} E_{nj}),
\end{aligned} \tag{37}$$

where $\Lambda = (\lambda_u, \ldots, \lambda_{n,m}) \geq 0$ representing the vector of dual variables adhering to the energy constraints of the proposed WSN. Therefore, the dual problem can be formulated as

$$\begin{aligned}
(P2): \quad & \max_{\Lambda} \; g(\Lambda) \\
& \text{subject to: } \Lambda \geq 0.
\end{aligned} \tag{38}$$

Dual function $g(\Lambda)$ is a concave function by definition since it has a point wise minimum of affine functions. ($\mathcal{L}(p, c_1, c_2, y, \beta, \alpha, \tau; \Lambda)$ is affine, i.e. linear, in (Λ)) [27]. Therefore, gradient or subgradient based methods can be used to solve the (P2) with guaranteed convergence. Then the subgradient of (36) can be written as

$$\Delta\lambda_u = E_u - \sum_{m=1}^{M} P_m^*(\Lambda)\frac{T(1-\alpha)(1-\beta)}{M}, \tag{39}$$

$$\Delta\lambda_{mn} = E_n^m - \sum_{j=1}^{M} P_j^*(\Lambda) d_{nj}^{\omega} |h_{n,j}|^2 T\alpha\tau, \tag{40}$$

where $\Delta\Lambda = (\Delta\lambda_u, \Delta\lambda_{m,1}, \ldots \Delta\lambda_{m,J})$. This updated method consists of polynomial computational complexity similar to the number of dual primal variables $(J+1)$, where $J = N/M$. Determining the optimal optimization variables in (36) realize the computation of the dual function. Thus, the dual function in (36) can be re-written as

$$g(\Lambda) \triangleq \min_{\substack{\mathbf{p} \in \mathcal{P}(c_1, c_2, y, \beta) \\ (c_1, c_2, y, \beta) \in \mathcal{D}}} \sum_{m=1}^{M}\sum_{n=1}^{J} \mathcal{L}_{2_{(m,n)}} + \lambda_u E_u + \sum_{m=1}^{M} \lambda_{mn} E_n^m, \tag{41}$$

where

$$\mathcal{L}_{2_{(n,m)}} \triangleq P_{out}^m - \lambda_u \sum_{m=1}^{M} P_m(\Lambda)\left(\frac{T(1-\alpha)(1-\beta)}{M}\right) - \sum_{m=1}^{J}\lambda_{mn}\sum_{j=1}^{M} P_j(\Lambda) d_{n,j}^{\omega} |h_{n,j}|^2 T\alpha\tau. \tag{42}$$

The optimal transmission power allocation of PB and CH over a given cluster of SNs can be ascertained by finding solutions for following formulated problem

$$(P3): \quad \min_{\Lambda} \ \mathcal{L}_{2_{(m,n)}} \quad \text{subject to: } P_m > 0 \ \& \ P_j > 0. \tag{43}$$

The function $\mathcal{L}_{2_{(m,n)}}$ is a concave function of P_j, P_m, where P_j denotes the transmission power of the PB and P_m denotes the transmission power of the CH in the cluster m. Hence, the optimal power allocations can be obtained by applying Karush-Kuhn-Tucker (KKT) conditions as in [27], [28]

$$P_m^* = P_j^*\left(1 + \frac{P_u |g_{mu}|^2 \eta_n \rho_u \gamma_2 \beta_m}{((1-\beta_m)\sigma_u^2 + \beta_m \kappa^2)}\right), \tag{44}$$

and

$$P_j^* = \left(\frac{\sigma_{nj}^2 \sigma_{mn}^2 d_{nj}^{-\omega}}{x(1-\tau)|h_{nj}|^2|h_{mn}|^2}\right) \times \left(\frac{(1-\tau)\gamma_1\alpha|h_{nj}|^2|h_{mn}|^2 - \lambda_u T\alpha\tau|h_{nj}|^2}{\lambda_u x + (1-\tau)\alpha\sigma_{nm}^2 M d_{mn}^{-\omega}}\right), \tag{45}$$

where

$$x = \sqrt{\frac{\lambda_{nm}(1-\tau)\alpha|h_{mn}|^2\sigma_{nj}^2}{\lambda_u |h_{nj}|^2 \sigma_{mn}^2}}. \tag{46}$$

It is also noteworthy that the dual variables λ_u and $\lambda_{m,n}$ affects the pricing scheme of the WSN in terms of economic perspective of the energy usage at the UAV and the PBs for RF-WPT technique. Next, substituting the optimal transmission power in (44) and (45) in (42), the transmission power variables can be eliminated from (42) and is denoted by $\mathcal{L}_{3_{(m,n)}}$. Then, by applying the changes into (41), an alternative version of the dual function can be expressed as

$$g(\Lambda) \triangleq \min_{\substack{\mathbf{p} \in \mathcal{P}(c_1, c_2, y, \beta) \\ (c_1, c_2, y, \beta) \in \mathcal{D}}} \sum_{m=1}^{M}\sum_{n=1}^{J} \mathcal{C}_{m,n} C_n^m \mathcal{L}_{3_{(m,n)}} + \lambda_u E_u + \sum_{m=1}^{M} \lambda_{mn} E_n^m. \tag{47}$$

Then, it is easily perceived that the optimal clustering and CH selection should be the one having minimum value for as $\mathcal{L}_{3_{(m,n)}}$ as

$$C_{mn}^* = \begin{Bmatrix} 1, & (m,n) = \arg\min \mathcal{L}_{3_{(m,n)}} \\ 0, & \text{otherwise} \end{Bmatrix}, \tag{48}$$

$$C_n^m = \begin{Bmatrix} 1, & n = \arg\min \mathcal{L}_{3_{(m,n)}} \\ 0, & \text{otherwise} \end{Bmatrix}, \tag{49}$$

$$T_n^m = \begin{Bmatrix} 1, & C_n^m = \arg\min \mathcal{L}_{3_{(m,n)}} \\ 0, & \text{otherwise} \end{Bmatrix}. \tag{50}$$

Hence, the function $\mathcal{L}_{3_{(m,n)}}$ works as the optimal criteria for clustering and CH selection under the threshold SNR values γ_1, γ_2 provided in the proposed system to maintained the expected QoS. Finally, by considering the values obtained in (48) and (49) substitute in $\mathcal{L}_{3_{(m,n)}}$ and adhering to the constraints (C1)(C3)(C6) in (35), the optimal value for β_m can be expressed as

$$\beta_m^* = \sum_{p=0}^{\infty}\left(\frac{\gamma_2^{\frac{p-1}{2}}\gamma_1 K_m^2(1-\alpha^*)\tau^*\alpha^*}{M H_{min}\eta_n(1-\gamma_1\kappa_m^2)}\right) \times K_{(v)}\left(2\sqrt{\frac{\gamma_1\gamma_2(1+p)\kappa_m^2\exp(-2K_m)}{\eta_n\Omega_{um}\Gamma(p+1)p!}}\right). \tag{51}$$

Finally, substituting(45) and (51) into (44) and considering (39),(40) and constraints (C1)(C2)(C3)(C4)(C5) in (35), the optimal values for τ and α can be expressed as

$$\tau^* = \frac{1}{\gamma_1}\left(\frac{\gamma_1 d_{nj}^{-\omega}\sigma_{nj}^2\alpha^*}{P_j|h_{nj}|^2} + \frac{T\alpha^* + |h_{nj}|^2}{M max(D)^{-\omega}}\right), \tag{52}$$

and

$$\alpha^* = \sum_{p=0}^{M}\left(\frac{[\gamma_1\gamma_2]^{(\frac{p-1}{2})} + T|h_{nj}|^2|h_{mn}|^2}{\max[D]^{\omega}\sum_{j=1}^{M} P_j\eta_n|h_{nj}|^2 M}\right) \times K_{(v)}\left(\frac{(1+K_m)}{\Omega_{mn}} \times \sqrt{\Omega_{mn}}\right). \tag{53}$$

By analyzing (53), it can be observed that γ_1 and γ_2 play a significant role in deciding α^*. Also it is noteworthy that the α^* is independent from the time ratios τ^* and β^*. However, τ^* in (52) depends on α^*, while β^* in (51) depends on both α^* and τ^*. This phenomena can be easily understand by analyzing (43) and (44) with respect to the Fig. 2. The computational complexity of the proposed asymptotic method is $\mathcal{O}(N \cdot M^5 \cdot J^2)$ considering the traveling salesman problem (TSP) for UAV trajectory. It is noteworthy that the the proposed asymptotic method is having a less time complexity compared to the traditional Brute-force search method of $\mathcal{O}(N^3 \cdot (N-J)! \cdot J \cdot M^6)^{N!}$ which is a NP-Hard problem [29].

VI. Low Complexity Heuristic Method

In this section, a low complexity sub optimal heuristic solution is proposed to solve (P1) in (35), while reducing the travelling distance of the UAV. Therefore, clustering and CH selection criteria that minimize the equivalent of (47) is given by the proposed algorithms to further reduce the time complexity.

The proposed clustering algorithm is illustrated in Algorithm 1. The proposed clustering technique presented as a modified version of K-mean clustering, where SNs are grouped around the PBs depending on the amount of energy harvested and minimum Euclidean distance to PBs. K-mean algorithm is a well known method used to partition N number of SNs into given number of clusters resulting the network in to Voronoi cells [30]. Apart from the nearest mean to the PBs, the amount of harvested energy and the uniform distribution of SNs within each clusters are considered in proposed Algorithm. After performing modified version of K-mean algorithm in Algorithm 1, we update the clusters to be end up with nearly equal in size by distorting the shape of the Veronoi cells. The algorithm starts by placing M number of PBs randomly and obtaining optimal transmission power allocations for PBs. Then PBs are considered as a center point for clustering (for K-mean clustering $K = M$) inside WSN. Next, by jointly considering the maximum amount of energy harvested out of PBs and the mean of the horizontal and vertical Euclidean distances to the PBs from the SN, each SN identifies its cluster. Even though SN satisfies the aforementioned requirements for clustering, if the selected cluster has already J number of SNs and a larger value for mean Euclidean distance to the PB, SN will be put into set Q_m, which will be used later to balance the size of the each cluster. This step is repeated until the size of each cluster is equals to J or $J+1$. Remaining part of the algorithm balance the size of each cluster until the cluster size is equal to J or $J+1$. The running time of the Algorithm 1 can be calculated in two phases. The running time of proposed modified K-mean algorithm is $\mathcal{O}(NMT_a)$, where T_a denotes the number of iterations until the convergence. The running time of the second phase of the algorithm is $\mathcal{O}(MJG\log(G))$. Thus, the time complexity of the Algorithm 1 can be given as $\mathcal{O}(NMT_a + MJG\log(G))$.

Convergence Proof of Algorithm 1: In time, the algorithm terminates after some iterations for the first phase, which performs initial clustering of SNs depending on the amount of energy harvested and characteristics of K-means algorithm. Due to the facts that the PBs act as the fixed central points for each clusters and after some iterations, completion of SN assignment are resulting convergence of the algorithm. For the phase two of the algorithm, if cluster size is not equals to J or $J+1$, then borrowing SNs from large size clusters algorithm terminates by balancing the clusters' sizes within the WSN. Also it is noteworthy that for each small size cluster there is at least one large size cluster according to the first phase of the algorithm.

The proposed heuristic method for CH selection and UAV trajectory is given in Algorithm 2. The clustering results

Algorithm 1 Clustering

Data:
- Sets N, M, A and T
- simulation based values of α, τ
- Optimal transmission power of PBs as in (44)

Result: sets A, A' set of clusters Q_m, $m = 1, 2, \ldots, M$, where $Q_m \in B$

Randomly placed PBs with locations $r_1, \ldots, r_m$ Initialize Q_m
SNs harvest energy from PBs
Phase I
for *each SN* $n \in S$ **do**
  if *n is active* **then**
    Add n into set A
  else
    Add n into set A'
  end
end
while *convergence* **do**
  for *each SN* $n \in A$ **do**
    for *each PB* m **do**
      if $E_{n,m}$ *is max* $\mathcal{E}_m$ **then**
        if *cluster size* $\leq J$ & $d_{m,n} \leq Q_m$ **then**
          $\| v_n - r_m \|^2 = \min\{\lambda_{3_{(m,n)}}\}$
          $Q_m \leftarrow (n)$
        else
          $\| v_n - r_m \|^2 = min\{\lambda_{3_{(m,n)}}\}$
          $Q_m \leftarrow (n)$
          $Q_{max} \leftarrow Add(n)$
        end
      else
        next iteration;
      end
    end
  end
  for *all clusters* m **do**
    $r_m = meanof\ Q_m$
  end
end
Phase II **while** *until cluster size* J *or* $J+1$ **do**
  for *all clusters* m **do**
    while *Cluster size* $< J$ **do**
      if *selected SN* $n^* \in Q_{max}$ & $size(m) > J$ **then**
        $Q_{max} \leftarrow Add(n^*)$ increase restricted level
      else if *selected SN* $n^* \in Q_{max}$ & *restricted level* $= 0$ **then**
        $Q_{max} \leftarrow Add(n^*)$ increase restricted level
      else
        selected SN $n^* = Q_{max}$ restricted level $\leq R_{max}$ $Q_{max} \leftarrow Add(n^*)$ increase restricted level
      end
    end
  end
end

obtained in Algorithm 1 is required to execute Algorithm 2. The algorithm considers the starting and ending points of the UAV when deciding the optimal CH for the given cluster. First, for a given q number of SNs, which are having the first highest amount of energy is added to the set E' and the Euclidean distance from each SN to UAV's direct trajectory is calculated. Then, the SN having the minimum distance to UAV's direct trajectory and SN which minimizes the (47) is selected as the CH. To decide the UAV trajectory, a well known Travelling salesman Problem (TSP) is used [29].

Algorithm 2 Cluster Head Selection & UAV Trajectory

Data:
- Sets S, A, B, E, and Q_m
- UAV starting(S) and ending points (D)

Result:
- Sets E' and Q_{CH}
- C_n^m, $n = 1, 2, \ldots, N \in A$ and $m = 1, \ldots, M \in B$
- Trajectory of the UAV

Phase I
Add q no of SNs with highest energy within Q_m to set E'_m, where $n \in (S \cap Q_m \cap A \cap E)$.
$L_{U_S,U_D} \leftarrow$ Draw a straight line between U_S and U_D
for *each cluster* $m \in B$ **do**
  for *each SN* $n \in (A \cap E'_m \cap Q_m)$ **do**
    Find $d_{L_{U_S,U_D}}$
  end
  for *each SN* $n \in (A \cap E' \cap Q_m)$ *in* **do**
    $C_n^m = \min(d_{L_{U_S,U_D}})$
    if $C_n^m = min\{\lambda_{3_{(m,n)}}\}$ **then**
      C_n^m =1
      $Q_{CH} \leftarrow C_n^m$
    else
      C_n^m =0
    end
  end
end
Phase II
$Q' = Q_{CH}$
$Z \leftarrow$ Find nearest CH to S from Q'
$Y_{S,Z} \leftarrow (S, Z)$
delete Z from Q'
while $Q' = \emptyset$ **do**
  $Z' \leftarrow$ find nearest CH to Z
  $Y_{Z,Z'} \leftarrow$ link(Z, Z')
  $Z = Z'$
  delete Z from Q'
end
$Y_{Z,D} \leftarrow$ link(Z, D)

The running time complexity of the Algorithm 2 can be calculated in two phases, clustering and UAV trajectory, respectively. The proposed method for clustering has the running time complexity of $\mathcal{O}(NM)$ and $\mathcal{O}(M^2)$ of time complexity similar to TSP in [29], where clustering takes more time to run than the time taken for finalizing UAV's trajectory.

TABLE II
SIMULATION PARAMETERS

Parameter	Value
SNR threshold values for successful transmission γ_1, γ_2 (dBm)	5
Transmission power of PBs P_j (dBm)	60 [31]
Transmission data rate of SNs R (bits/sec/Hz)	2
pathloss exponent ω	2.4
constant co-efficient of pathloss κ	1.3
Ricean K-factor K	2.25
energy conversion efficiency at SNs η	0.8
Total operational time T (Sec.)	100
Noise power between SNs $\sigma^2_{n,m}$ (dBm)	-80
Noise power between CH and the UAV $\sigma^2_{u,m}$(dBm)	-150
UAV altitude $H_{min}(m)$	100

Thus, the total time complexity of the Algorithm 2 is can be given as $\mathcal{O}(NM)$. Similarly, the time complexity of the Algorithm 1 can be given as $\mathcal{O}(NMT_\alpha)$ since modified K-mean algorithm run time is higher than the cluster balancing. Therefore, the proposed heuristic method shows a greater advantage of computational time complexity of $\mathcal{O}(NMT_\alpha + NM)$ compare to traditional Brute-force search method of $\mathcal{O}(N^3 \cdot (N-J)! \cdot J \cdot M^6)$ and also better than the proposed asymptotic method of $\mathcal{O}(N \cdot M^5 \cdot J^2)$.

Convergence Proof of Algorithm 2: The convergence of CH selection phase in the algorithm is easy to prove since computing euclidean distance to UAV's direct trajectory and selecting SN from max energy vector(E'_m) are straightforward mathematical computations. Thus, the phase I of the algorithm terminates easily when the one CH is selected. For each iteration of phase II, one CH is assigned to the UAV's trajectory adhering to the constraints given in (30)-(34). Thus, the phase II of the algorithm will eventually terminates since the number of CHs is finite and equal to number of PBs in the proposed context.

VII. SIMULATION RESULTS

In this section, simulation results are provided to evaluate the performance of the proposed wireless powered UAV-aided WSN. Unless otherwise stated, 10 different WSN setups have been used for the simulations, where $N = 50, 100, 150, \ldots, 500$ and SNs are randomly distributed over the area of $N \times Nm^2$. In addition, M number of PBs are randomly placed within the area of WSN. The number of PBs are set to $N/0.2$, which is proved and analyzed via subsequent simulation results. The both starting and ending of the UAV are placed randomly within $1 - 50$ m away from the edges of the WSN such that the direct line between the points is crossing the WSN. Unless otherwise stated, the values used in simulations are given in Table II. The maximum battery capacity of the SNs E_{max} is set to ≈ 15 Wh [32].[4]

[4]SNs have high capacity batteries such as dry cell (D) batteries (15000 mAh) comparing to with the widely used AA batteries ($2000 \sim 2400$ mAh) [32].

TABLE III

OUTAGE PROBABILITY OF THE PROPOSED SYSTEM WITH RESPECT TO TIME RATIO α, τ, β

$\tau = 0.3$				
$\beta \vert \alpha$	0.5	0.6	0.7	0.8
0.1	0.1059	0.1032	0.1642	0.2956
0.2	0.0881	**0.0854**	0.1913	0.4409
0.3	0.1494	0.1253	0.1037	0.1274
0.4	0.1317	0.1165	0.1133	0.1119
0.5	0.1398	0.1234	0.1196	0.1166
0.6	0.3354	0.1991	0.1839	0.7277
0.7	0.4398	0.3323	0.4271	0.6321

$\tau = 0.4$				
$\beta \vert \alpha$	0.5	0.6	0.7	0.8
0.1	0.0759	0.0732	0.1343	0.2657
0.2	0.0582	**0.0553**	0.1633	0.4109
0.3	0.1195	0.0953	0.0737	0.0975
0.4	0.1017	0.0865	0.0833	0.0819
0.5	0.1098	0.0939	0.0896	0.0866
0.6	0.3055	0.1991	0.1539	0.6977
0.7	0.4098	0.3029	0.3970	0.5921

$\tau = 0.5$				
$\beta \vert \alpha$	0.5	0.6	$= 0.7$	0.8
0.1	0.1260	0.1232	0.1842	0.3156
0.2	0.1082	**0.1054**	0.2133	0.4609
0.3	0.1695	0.1453	0.1237	0.1474
0.4	0.1517	0.1365	0.1333	0.1319
0.5	0.1598	0.1439	0.1396	0.1365
0.6	0.3555	0.2491	0.2039	0.7477
0.7	0.4598	0.3529	0.4471	0.6421

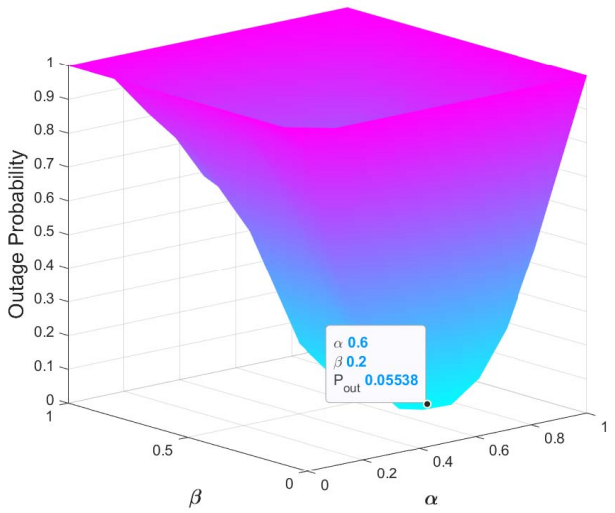

Fig. 3. Outage probability of the proposed system with respect to α, β, τ, where $N = 100$. Due the limitations in representation, τ is presented in TABLE III.

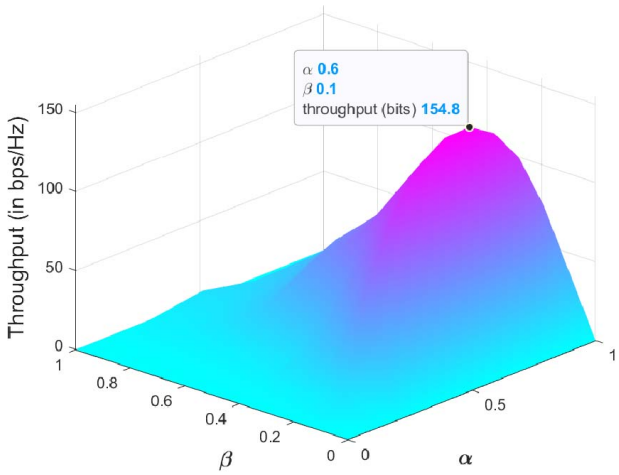

Fig. 4. Achievable throughput of the proposed system with respect to α, β, τ, where $N = 100$. Due to the limitations in representation, τ is presented in the figure.

Fig. 3 depicts the influence of time ratios α, τ, β on the end-to-end outage probability of the proposed system. The objective of this simulation is to identify optimal time ratios that minimize the outage probability. Due to the limitations in representation, τ is not presented in the Fig. 3. Thus, Table III is provided with the corresponding outage probability values with respect to α, τ, β. It can be observed from the both Table III and Fig. 3 that the combination of optimal values of α, τ, β that achieves lowest outage probability at 0.0553 equals to 0.6, 0.4, 0.2. Also, it is observed from Table III that when $\tau \neq 0.4$, the outage probability increase for every combination of α, β. This observation makes sense since τ decides the amount of time allocation for EH via RF-WPT in Phase-I. If τ is larger, there is not enough time for information transmission between SNs and CHs and if τ is smaller, not enough energy is harvested at SNs leading to poor transmission power. In either case, outage probability increases regardless of the combination of α, β. Moreover, it is also noted from the Table III that regardless of τ, when β increases α also increases up to 0.8 and then decreases to maintain low outage probability. This make sense since the time allocation for information transmission between CH and UAV is critical to maintain lower outage probability. The analytical values of α, β, τ obtained from (53),(51) and (52) of the proposed asymptotic method are 0.6458, 0.2114, 0.4499, respectively. Analytically obtained time ratios approximately equals to the simulation results shown in Table III and Fig. 3 proving the accuracy of proposed asymptotic method, and it achieves local optimality.

Fig. 4 demonstrates the influence of time ratios on the achievable sum throughput at the data sink. It is can clearly be seen from Fig. 4 that there exists an optimal values for time ratios similar to Fig. 3. This observation makes sense since the outage probability in (18) directly affects the sum throughput as in (20). According to the results shown in Fig. 4, maximum sum throughput is always achieved when the combination of time ratios (α, τ, β) equals to 0.6, 0.1, 0.4. However, it is worth mentioning that the value of $\beta = 0.1$ is different from the optimal value of $\beta = 0.2$ in Fig. 3. Understanding of this result is straightforward since the weight of the aggregated data transmitted by CHs is heavier than the data transmitted by SN. Thus, more time need to be allocated for data transmission between CH and the UAV to achieve higher sum-throughput according to (20). Jointly considering Fig. 3 and Fig. 4 it is worth claiming that the optimal value for α, τ should be 0.6 and 0.4, respectively and the value of β has to be selected out of the values 0.1 and 0.2, when $E_n^m < E_{max}$ depending on the QoS requirement of the system.

The outage probability at the data sink for different number of SNs versus number of clusters in proposed system is illustrated in Fig. 5. Both analytical and simulation based optimal values of time ratios are used to obtain the results shown in Fig. 5. Further, it can be clearly observed from Fig. 5,

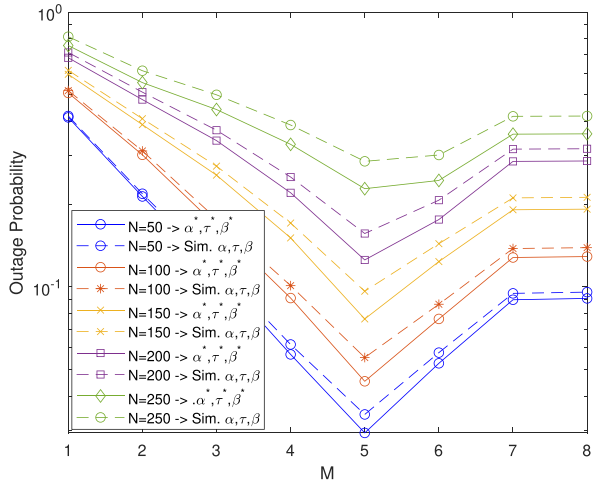

Fig. 5. Outage probability for different number of SNs versus number of clusters in proposed WSN. The both asymptotic and simulation based optimal values for time ratios (α, β, τ) are used in the simulation.

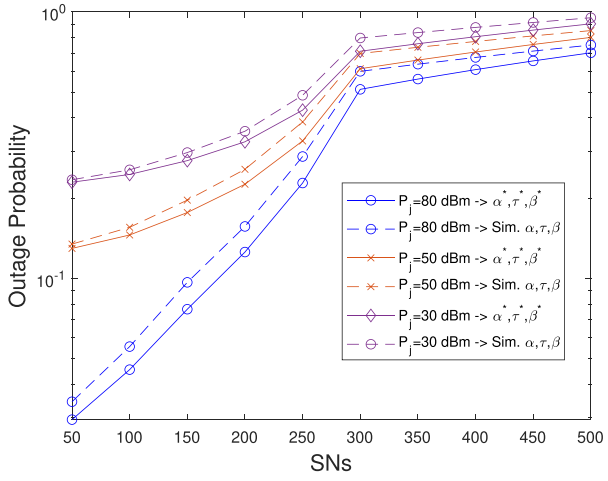

Fig. 6. Outage probability for different transmission powers of PBs versus number SNs in WSN.

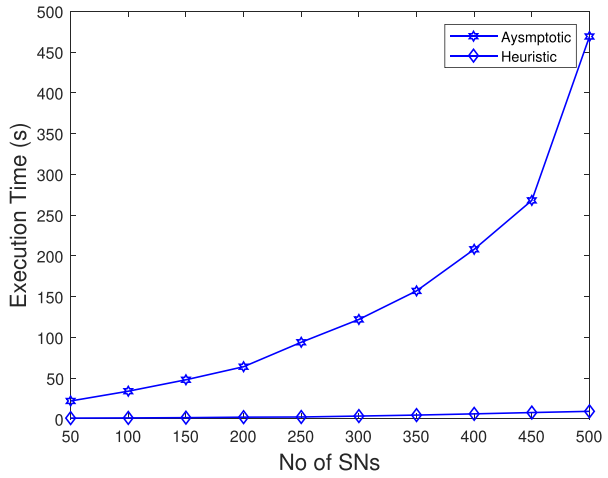

Fig. 7. Execution time for proposed asymptotic and heuristic methods versus number of SN in the WSN.

that regardless of the number of SNs, the minimum outage probability is always achieved when the number of clusters equals to 5, claiming that 20% of the SNs should be in one cluster. Thus, in order to achieve optimal results for the outage probability, $M = N \times 0.2$ PBs are needed in the proposed system setup. In addition, analytically obtained optimal time ratios are shown superior outage probability compared to numerically obtained optimal values and the outage probability difference between analytical and numerical optimal values are increasing with the increase in number of SNs in the proposed WSN.

The outage probability for different transmission powers of PBs with respect to the number of SNs in WSN is depicted in Fig. 6. As it can be clearly seen from Fig. 6, regardless of the number of SNs in the system, $P_j = 80$ dBm always achieves the lowest outage probability. Moreover, similar to Fig. 5, optimal time ratios obtained analytically show the superior outage performance compared to optimal values obtained through the simulations. However, with the increase in transmission power of PBs and number of SNs in the proposed system, the outage probability decrease illustrating maximum capacity of the number of SNs in the proposed system, which is equals to around $250 - 300$.

Execution time[5] of the proposed asymptotic and heuristic methods are shown in the Fig. 7. The proposed asymptotic method obtains optimal solutions in 24 to 478 seconds depend on the number of SNs, while low complexity heuristic method obtains solutions under 15 seconds. Conversely, the Brute-force method takes more than 19 hours to obtain results for the given WSN. Thus, these results confirm that the proposed asymptotic and heuristic method is much lower in complexity than the traditional Brute-force search method. It also noteworthy that the proposed heuristic method is much better than the proposed asymptotic method in terms of execution time complexity.

[5]Note that the execution time can be varying according to the system specification of the computer and the versions of application software(i.e,MatLab) running the simulation.

Fig. 8 depicts the input and output of the proposed WSN. Fig. 8a shows the initial stage of the proposed WSN, where 100 SNs are randomly distributed in the area of $100 \times 100m^2$ with M number of randomly distributed PBs. Fig. 8b illustrates the output result of the proposed system after the Phase I, where SNs are clustered into M number of clusters having 20% SNs per each cluster. And then, CH per each cluster is selected according to the proposed optimal methods considering the UAVs direct trajectory. Fig. 8c shows the same scenario similar to Fig. 8a with different starting and ending locations of the UAV. It is clearly can be seen from Fig. 8a that the selected CHs are different as compared to Fig. 8b in order to accommodate the changes in UAV's trajectory.

The sum throughput versus transmission power of PBs are shown in Fig. 9 to compare the performance of proposed asymptotic and heuristic methods with the traditional Brute-force search. Due to the execution complexity of Brute-force search for larger number of SNs ($N \geq 20$), two simulation results are given for better comparison of the proposed asymptotic and heuristic methods. It can be observed from the Fig. 9a that the proposed asymptotic method shows

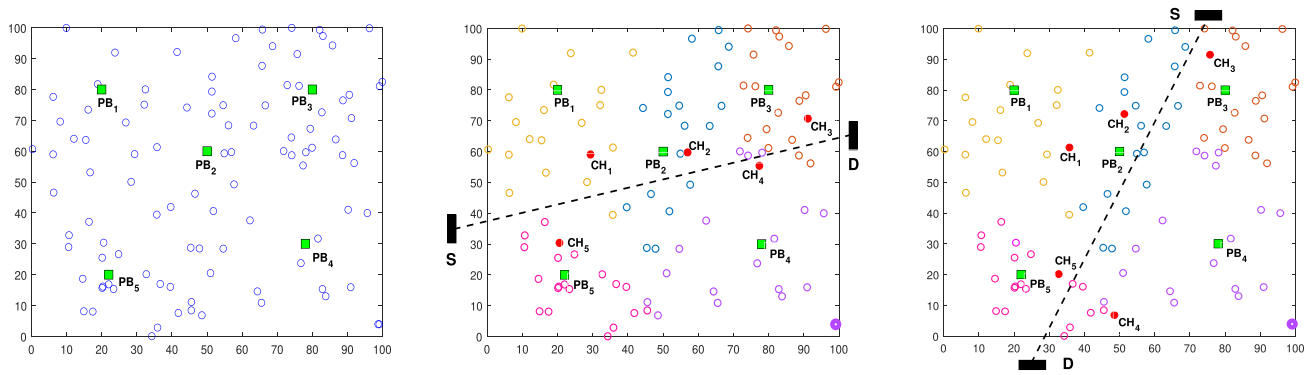

Fig. 8. (a) Sample input network topology for low complexity heuristics method, where $N = 100$ and $M^* = 5$. (b) Output network topology of low complexity heuristics method when S and D of the UAV are located in west and east side of the network, respectively. (c) Output network topology of low complexity heuristics method when S and D of the UAV are located in north and south side of the network, respectively.

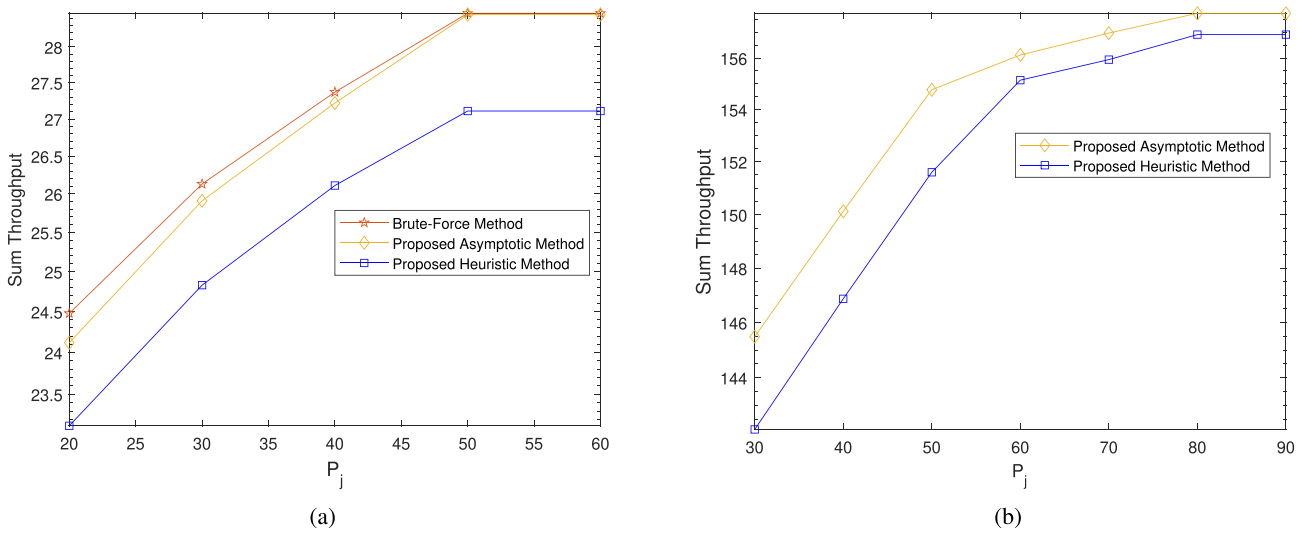

Fig. 9. Sum throughput achieved by the proposed system with respect to difference transmission power of the PB for comparison of the algorithms. (a) WSN with $N = 20$ due to the high complexity of Brute-force method, which is unable to realize for higher number of SNs. (b) WSN with $N = 100$ using the general parameters as in TABLE II.

approximately close performance as Brute-force search with higher transmission power of PBs. However, in lower transmission powers of PBs primal solution of the Brute-force method shows significant superiority having a duality gap between primal and proposed asymptotic method. On the other hand, the proposed heuristic method shows inferior performance compared to the proposed asymptotic method. Since Fig. 9a alone is not enough to claim the performance difference between proposed asymptotic and heuristic methods, sum throughput versus transmission power of PBs in WSN with 100 SNs is given in Fig. 9b. The proposed asymptotic methods still show the superior performance compared to the proposed heuristic method. However, increase in transmission power of PB reduces the performance gap between the proposed asymptotic and heuristic methods.

Finally, the sum-throughput performance of the proposed asymptotic and heuristic methods with respect to baseline WSNs are illustrated in Fig. 10. Two baseline systems are used with similar parameters as mentioned in Table II to make a fare comparison, i.e. (1). UAV-aided WSN without WPT, (2) WSN without UAV and RF-WPT, in which CHs are directly communicating with the data sink. As it can clearly seen from the Fig. 10, the both proposed asymptotic and heuristic methods show superiority in achievable sum-throughput at data sink compared to baseline WSNs. The proposed asymptotic method shows 41.44% performance gain as compared to traditional WSN without UAV and RF-WPT, while the proposed heuristic method shows 39.63% performance gain in terms of achievable sum-throughput. In addition, the proposed asymptotic and heuristic method shows 8.27% and 6.89% performance gain in terms of sum-throughput at data sink, respectively with comparison to UAV-assisted WSN without RF-WPT. The relative sum-throughput performance gain of the proposed asymptotic and heuristic methods compared to baseline WSNs is given in Table IV.

Jointly considering all the simulation results provided in this section, it is worth claiming that the proposed RF-WPT enabled UAV-assisted WSN is showing significant

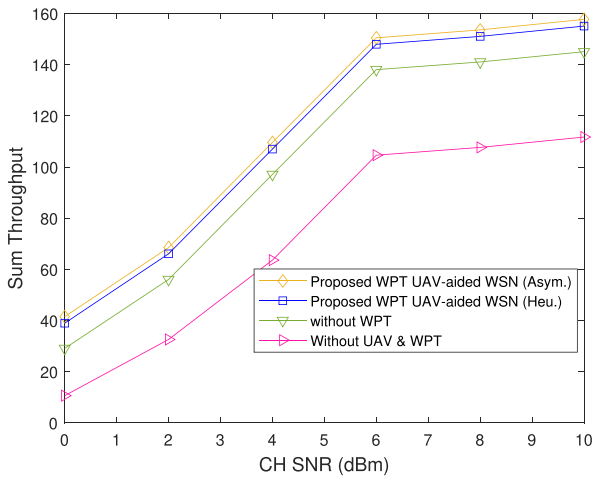

Fig. 10. Sum-throughput versus transmission SNR of CH for comparison of the proposed asymptotic and heuristic methods with baseline systems.

TABLE IV

THE RELATIVE PERFORMANCE GAIN IN TERMS OF ACHIEVABLE SUM-THROUGHPUT OF THE PROPOSED ASYMPTOTIC AND HEURISTIC METHODS. CONVENTIONAL WSN IS TREATED AS THE BASELINE SCHEME

#	System Model	Performance Gain (Relative)
1	Conventional WSN	1%
2	UAV-aided WSN	28.75%
3	WPT+ UAV-aided WSN (proposed heuristic method)	34.02 %
4	WPT+ UAV-aided WSN (proposed asymptotic method)	35.90 %

performance gain compared to baseline WSN system models within the given simulation setup presented in Table II. It is also identified that the maximum limit for sum throughput achieved when the transmission power of PBs $P_j = 80dBm$. Further increase in P_j has no effects on the system performance of the proposed system. The proposed RF-WPT enabled UAV-assisted WSN is a well designed candidate for any UAV-assisted IoT applications such as intelligent transportation systems in automotive industry, smart cities, agriculture automation etc.

VIII. CONCLUSION

In this paper, a new resource allocation and UAV aided data collection is proposed for wireless powered UAV-assisted WSN over multiple fading channels, i.e. Rayleigh and Rician fading. All the SNs are powered using randomly placed PBs and then SNs periodically send its sensed data to selected CHs to be collected by the UAV. A new time block structure is proposed to accommodate all the operations of the proposed WSN. Due to the complexity of the formulated outage minimization problem, Lagrangian duality is used to solve the problem with polynomial complexity compared to traditional NP-hard Brute-force search method. Additionally, a heuristic algorithm is proposed by decomposing the problem into sub problems; clustering and CH selection to minimize the computational complexity. Simulation results revealed the superiority of the proposed methods as compared to other benchmark schemes in general. The proposed RF-WPT enabled UAV-aided WSN can be used to collect more information from infrastructures of transportation systems, i.e, railways, roads, etc. to have better condition monitoring for ITS applications.

REFERENCES

[1] T. Liu, X. Wang, and L. Zheng, "A cooperative SWIPT scheme for wirelessly powered sensor networks," *IEEE Trans. Commun.*, vol. 65, no. 6, pp. 2740–2752, Jun. 2017.

[2] T. D. Ponnimbaduge Perera, D. N. K. Jayakody, S. K. Sharma, S. Chatzinotas, and J. Li, "Simultaneous wireless information and power transfer (SWIPT): Recent advances and future challenges," *IEEE Commun. Surveys Tuts.*, vol. 20, no. 1, pp. 264–302, 1st Quart., 2018.

[3] Y. Zhang, S. He, J. Chen, Y. Sun, and X. S. Shen, "Distributed sampling rate control for rechargeable sensor nodes with limited battery capacity," *IEEE Trans. Wireless Commun.*, vol. 12, no. 6, pp. 3096–3106, Jun. 2013.

[4] S. Riviere, A. Douyere, F. Alicalapa, and J. D. L. S. Luk, "Study of complete WPT system for WSN applications at low power level," *Electron. Lett.*, vol. 46, no. 8, pp. 597–598, Apr. 2010.

[5] T. Ajmal, D. Jazani, and B. Allen, "Design of a compact RF energy harvester for wireless sensor networks," in *Proc. IET Conf. Wireless Sensor Syst. (WSS)*, Jun. 2012, pp. 1–5.

[6] L. Sun, L. Wan, K. Liu, and X. Wang, "Cooperative-evolution-based WPT resource allocation for large-scale cognitive industrial IoT," *IEEE Trans. Ind. Informat.*, vol. 16, no. 8, pp. 5401–5411, Aug. 2020.

[7] D. Belo, D. C. Ribeiro, P. Pinho, and N. B. Carvalho, "A selective, tracking, and power adaptive far-field wireless power transfer system," *IEEE Trans. Microw. Theory Techn.*, vol. 67, no. 9, pp. 3856–3866, Sep. 2019.

[8] N. Aslam, K. Xia, and M. U. Hadi, "Optimal wireless charging inclusive of intellectual routing based on SARSA learning in renewable wireless sensor networks," *IEEE Sensors J.*, vol. 19, no. 18, pp. 8340–8351, Sep. 2019.

[9] L. Wang, H. Shao, J. Li, X. Wen, and Z. Lu, "Optimal multi-user computation offloading strategy for wireless powered sensor networks," *IEEE Access*, vol. 8, pp. 35150–35160, 2020.

[10] P. Kumar, S. Garg, A. Singh, S. Batra, N. Kumar, and I. You, "MVO-based 2-D path planning scheme for providing quality of service in UAV environment," *IEEE Internet Things J.*, vol. 5, no. 3, pp. 1698–1707, Jun. 2018.

[11] S. Garg, A. Singh, S. Batra, N. Kumar, and L. T. Yang, "UAV-empowered edge computing environment for cyber-threat detection in smart vehicles," *IEEE Netw.*, vol. 32, no. 3, pp. 42–51, May 2018.

[12] S. Garg, G. S. Aujla, N. Kumar, and S. Batra, "Tree-based attack–defense model for risk assessment in multi-UAV networks," *IEEE Consum. Electron. Mag.*, vol. 8, no. 6, pp. 35–41, Nov. 2019.

[13] T. Shen and H. Ochiai, "A UAV-aided data collection for wireless powered sensor network over Rician fading channels," in *Proc. 16th IEEE Annu. Consum. Commun. Netw. Conf. (CCNC)*, Jan. 2019, pp. 1–5.

[14] C. Zhan, Y. Zeng, and R. Zhang, "Energy-efficient data collection in UAV enabled wireless sensor network," *IEEE Wireless Commun. Lett.*, vol. 7, no. 3, pp. 328–331, Jun. 2018.

[15] S. Say, H. Inata, J. Liu, and S. Shimamoto, "Priority-based data gathering framework in UAV-assisted wireless sensor networks," *IEEE Sensors J.*, vol. 16, no. 14, pp. 5785–5794, Jul. 2016.

[16] J. Gong, T.-H. Chang, C. Shen, and X. Chen, "Aviation time minimization of UAV for data collection from energy constrained sensor networks," in *Proc. IEEE Wireless Commun. Netw. Conf. (WCNC)*, Apr. 2018, pp. 1–6.

[17] L. Zhao, S. Qu, and Y. Yi, "A modified cluster-head selection algorithm in wireless sensor networks based on LEACH," *EURASIP J. Wireless Commun. Netw.*, vol. 2018, no. 1, p. 287, Dec. 2018, doi: 10.1186/s13638-018-1299-7.

[18] A. Sarkar and T. Senthil Murugan, "Cluster head selection for energy efficient and delay-less routing in wireless sensor network," *Wireless Netw.*, vol. 25, no. 1, pp. 303–320, Jan. 2019, doi: 10.1007/s11276-017-1558-2.

[19] T. M. Behera, S. K. Mohapatra, U. C. Samal, M. S. Khan, M. Daneshmand, and A. H. Gandomi, "Residual energy-based cluster-head selection in WSNs for IoT application," *IEEE Internet Things J.*, vol. 6, no. 3, pp. 5132–5139, Jun. 2019.
[20] H.-V. Tran and G. Kaddoum, "RF wireless power transfer: Regreening future networks," *IEEE Potentials*, vol. 37, no. 2, pp. 35–41, Mar. 2018.
[21] V. J. Hodge, S. O'Keefe, M. Weeks, and A. Moulds, "Wireless sensor networks for condition monitoring in the railway industry: A survey," *IEEE Trans. Intell. Transp. Syst.*, vol. 16, no. 3, pp. 1088–1106, Jun. 2015.
[22] N. P. Le, "Throughput analysis of power-beacon-assisted energy harvesting wireless systems over non-identical Nakagami-*m* fading channels," *IEEE Commun. Lett.*, vol. 22, no. 4, pp. 840–843, Apr. 2018.
[23] D. Ebrahimi and C. Assi, "On the interaction between scheduling and compressive data gathering in wireless sensor networks," *IEEE Trans. Wireless Commun.*, vol. 15, no. 4, pp. 2845–2858, Apr. 2016.
[24] C. You and R. Zhang, "3D trajectory optimization in Rician fading for UAV-enabled data harvesting," *IEEE Trans. Wireless Commun.*, vol. 18, no. 6, pp. 3192–3207, Jun. 2019.
[25] D. N. K. Jayakody, T. D. P. Perera, A. Ghrayeb, and M. O. Hasna, "Self-energized UAV-assisted scheme for cooperative wireless relay networks," *IEEE Trans. Veh. Technol.*, vol. 69, no. 1, pp. 578–592, Jan. 2020.
[26] S. Panic, M. Stefanovic, J. Anastasov, and P. Spalevic, *Fading and Interference Mitigation in Wireless Communications*. Boca Raton, FL, USA: CRC, 2013.
[27] D. Knowles, "Lagrangian duality for dummies," Stanford.edu, Stanford, CA, USA, Tech. Rep., Nov. 2010. [Online]. Available: https://www-cs.stanford.edu/~davidknowles/lagrangian_duality.pdf
[28] S. Boyd, S. P. Boyd, and L. Vandenberghe, *Convex Optimization*. Cambridge, U.K.: Cambridge Univ. Press, 2004.
[29] J. Ny, E. Feron, and E. Frazzoli, "On the dubins traveling salesman problem," *IEEE Trans. Autom. Control*, vol. 57, no. 1, pp. 265–270, Jan. 2012.
[30] M. Mahajan, P. Nimbhorkar, and K. Varadarajan, "The planar k-means problem is NP-hard," *Theor. Comput. Sci.*, vol. 442, pp. 13–21, Jul. 2012.
[31] Series 1000-Watt NDB Transmitter. (2020). *Southern Avionics Company, Leaders in Non Directional Beacon and Differential GPS Transmitters*. Accessed: Jun. 10, 2020. [Online]. Available: https://www.southernavionics.com/se-series-1000-watt-ndb
[32] G. Tuna and V. C. Gungor, "Energy harvesting and battery technologies for powering wireless sensor networks," in *Industrial Wireless Sensor Networks*. Amsterdam, The Netherlands: Elsevier, 2016, pp. 25–38.

Tharindu Dilshan Ponnimbaduge Perera (Graduate Student Member, IEEE) received the B.Sc. degree (Hons.) in software engineering and the M.Sc. degree from the Department of Computing, Faculty of ACES, Sheffield Hallam University, U.K. He is currently pursuing the Ph.D. degree in computer science and wireless communications with the Infocomm Lab, School of Computer Science and Robotics, National Research Tomsk Polytechnic University, Russia. He has been awarded a full-time scholarship from the Ministry of Education, Russian Federation for Ph.D. studies. Also, he is working as a Research Engineer with the Department of IT, School of Computer Science and Robotics, National Research Tomsk Polytechnic University. His research interests include simultaneous wireless information and power transfer, interference exploitation in RF energy harvesting, and UAV-assisted communication.

Stefan Panic (Member, IEEE) received the M.Sc. and Ph.D. degrees in electrical engineering from the Faculty of Electronic Engineering, Nis, Serbia, in 2007 and 2010, respectively. He is currently an Associated Professor with the Department of Informatics, Faculty of Natural Science and Mathematics, University of Pristina. He has published over 40 SCI indexed articles. His research interests in mobile and multichannel communications include statistical characterization and modeling of fading channels, performance analysis of diversity combining techniques, and outage analysis of multiuser wireless systems subject to interference. Within digital communication, his current research interests include the information theory, source and channel coding, and signal processing.

Dushantha Nalin K. Jayakody (Senior Member, IEEE) received the Ph.D. degree in electronics, electrical, and communications engineering from University College Dublin, Ireland, in 2013. From 2014 to 2016, he was a Postdoctoral Research Fellow with the Institute of Computer science, University of Tartu, Estonia, and the Department of Informatics, University of Bergen, Norway. Since 2016, he has been a Professor with the School of Computer Science and Robotics, National Research Tomsk Polytechnic University (TPU), Russia. In addition, since 2019, he also serves as the Dean of the School of Postgraduate and Research, Sri Lanka Technological Campus (SLTC), Padukka, Sri Lanka, and the Founding Director of the Centre of Telecommunication Research, SLTC. He has received the Best Paper Award from the IEEE International Conference on Communication, Management and Information Technology (ICCMIT) in 2017 and International Conference on Emerging Technologies of Information and Communications, Bhutan, in March 2019. In July 2019, he received the Education Leadership Award from the World Academic Congress in 2019. In 2017 and 2018, he received the Outstanding Faculty Award by National Research Tomsk Polytechnic University, Russia. He also received Distinguished Researcher in Wireless Communications, Chennai, India, in 2019. He has published over 140 international peer reviewed journals and conference papers and books. His research interests include PHY and NET layer prospective of 5G communications technologies such as NOMA for 5G etc., cooperative wireless communications, device to device communications, LDPC codes, and Unmanned Ariel Vehicle. He has organized or co-organized more than 20 workshops and special sessions of various IEEE conferences. He also served as the Chair, Session Chair or Technical Program Committee Member for various international conferences, such as IEEE PIMRC 2013-2019, IEEE WCNC 2014-2018, and IEEE VTC 2015-2018. He currently serves as an Area Editor of *Elsevier Physical Communications Journal, MDPI Information* journal, and *Wiley Internet of Technology Letters*. Also, he serves as a reviewer for various IEEE Transactions and other journals.

P. Muthuchidambaranathan (Member, IEEE) received the B.Eng. degree in electronics and communication engineering from the Government College of Technology, Coimbatore, India, in 1992, the M.Eng. degree in microwave and optical engineering from the A. C. College of Engineering and Technology, Karaikudi, India, in 1994, and the Ph.D. degree in optical communication from the National Institute of Technology (NIT), Tiruchirappalli, India, in 2009. He is currently working as an Associate Professor with the Department of Electronics and Communication Engineering, National Institute of Technology (NIT), Tiruchirappalli. His research interests include wireless communications and optical communications. He published his research papers in refereed international journals, and international and national conferences. He is an author of the textbook *Wireless Communications* (published by Prentice Hall of India).

Jun Li (Senior Member, IEEE) received the Ph.D. degree in electronic engineering from Shanghai Jiao Tong University, Shanghai, China, in 2009. From January 2009 to June 2009, he worked at the Department of Research and Innovation, Alcatel Lucent Shanghai Bell, as a Research Scientist. From June 2009 to April 2012, he was a Postdoctoral Fellow with the School of Electrical Engineering and Telecommunications, University of New South Wales, Australia. From April 2012 to June 2015, he was a Research Fellow with the School of Electrical Engineering, The University of Sydney, Australia. Since June 2015, he has been a Professor with the School of Electronic and Optical Engineering, Nanjing University of Science and Technology, Nanjing, China. He was a Visiting Professor with Princeton University from 2018 to 2019. His research interests include network information theory, game theory, distributed intelligence, multiple agent reinforcement learning, and their applications in ultradense wireless networks, mobile edge computing, network privacy and security, and industrial Internet of things.